



# Sediment source apportionment following wildfire in an upland commercial forest catchment

Enrique Muñoz-Arcos<sup>1</sup> · Alejandra Castillo<sup>1</sup> · Alicia Cuevas-Aedo<sup>1</sup> · Luis Ovando-Fuentealba<sup>2</sup> · Alex Taylor<sup>2</sup> · Ramón Bustamante-Ortega<sup>3</sup> · William H. Blake<sup>2</sup> · Claudio Bravo-Linares<sup>1</sup>

Received: 27 October 2020 / Accepted: 2 April 2021 / Published online: 10 April 2021  
© The Author(s), under exclusive licence to Springer-Verlag GmbH Germany, part of Springer Nature 2021

## Abstract

**Purpose** Wildfires can have major impacts on water scarcity and water quality linked to off-site transfer of polluting ash and nutrients. Understanding sediment sources in burnt landscapes can help to develop mitigation strategies, especially in catchments planted with introduced species that are prone to fire. We investigated sediment sources activated by post-fire rainfall in a small-forested catchment that was impacted by a severe wildfire. The aim was to use environmental radionuclides and elemental geochemistry as tracers to apportion sediment sources within burnt plantation systems.

**Methods** Surficial (0–2 cm) topsoil ( $n = 9$ ), sub-surficial (2–4 cm) topsoil (i.e. below the burnt layer;  $n = 8$ ) samples from burnt hillslopes and forest roads ( $n = 5$ ) and stream banks ( $n = 5$ ) soil samples were taken in the Quivolgo catchment, El Maule region, Chile. Sediment samples ( $n = 9$ ) were collected from behind a v-notched weir on three dates after the fire: May 2017, July 2017 and October 2017. Soil and sediment samples were analysed by gamma spectrometry and wavelength-dispersive X-ray fluorescence (WD-XRF) used to obtain tracer properties. These were evaluated visually and statistically to identify potential non-conservative tracers. Sediment apportionment was undertaken using the MixSIAR mixing model.

**Results** The tracer selection procedure resulted in ten tracers being used for sediment apportionment. Tracer suitability was based on (i) weak and non-significant linear relationship between tracer concentrations and specific surface area (SSA) and soil organic matter (SOM), and (ii) conservative behaviour supported by the inclusion of sediment samples within source convex hull. Sediments from sub-surface layer (2–4 cm) were the dominant source during the first two periods contributing  $55 \pm 11$  and  $78 \pm 10\%$  respectively, whereas road contribution was only important in the last period ( $71 \pm 14\%$ ). Apportionment showed a shift in sediment source (i.e. from forest roads to hillslopes) compared to a previous study in the same catchment before wildfire. The main driver of erosion was attributed to overland flow convergence and consequent rill erosion across burnt hillslopes.

**Conclusion** The study demonstrated combined use of environmental radionuclides with elemental geochemistry for sediment apportionment within burnt forest plantations and highlighted a switch in predominant source (e.g. sub-surface burnt soil) activated by post-fire rainfall events. The findings in this research will help forest companies to develop strategies to reduce off-site impacts of sediment release after wildfire in forest plantations.

**Keywords** Sediment fingerprinting · Wildfires · Forest plantations · Post-fire sediment sources · MixSIAR

---

Responsible editor: Hugh Smith

---

✉ Claudio Bravo-Linares  
cbravo@uach.cl

<sup>1</sup> Facultad de Ciencias, Instituto de Ciencias Químicas, Universidad Austral de Chile, Independencia, 641 Valdivia, Chile

<sup>2</sup> School of Geography, Earth and Environmental Sciences, University of Plymouth, Plymouth, Devon PL4 8AA, UK

<sup>3</sup> Centro de Información de Recursos Naturales (CIREN), Av. Manuel Montt, 1164 Santiago, Chile

## 1 Introduction

An estimated 7.20 billion ha of land were burnt between 2001 and 2018 at an average rate of more than 400 million ha per year (FAO 2020). Wildfires pose a threat to life and property, particularly at the urban/forest interface. In addition, wildfires can assert pressure on water resource availability and quality (Martin 2016) linked to off-site transfer of polluting ash and nutrients (Blake et al. 2010). This underpins the need for a process understanding of hillslope and channel connectivity in burnt landscapes (Wilkinson et al. 2009).

Wildfires have been recognised as an important cause of hydrological and geomorphological changes over short and long timescales (Shakesby and Doerr 2006). Depending on its severity, wildfires can remove some or all of the vegetation and litter cover, thereby affecting transpiration, interception, surface storage capacity for rain and obstacles to overland flow (Shakesby and Doerr 2006). In parallel, remaining ashes can have substantial effects on soil physical and chemical properties, nutrient cycles, carbon (C) cycle, hydrological processes, water quality, microbial activity and plant growth (Bodi et al. 2014). Moreover, there are a number of additional factors that can affect post-fire erosion such as slope, fire severity and vegetation status after fire that can cause divergent responses in erosion rates and sediment yields (Shakesby and Doerr 2006). In the post-fire context, rainfall ranks as the most important driver of runoff and erosion caused mainly by changes in soil moisture, structure and infiltration which can accelerate sediment transport and deposition (Ice et al. 2004; Moody et al. 2013; Shakesby et al. 2016). Hence, increased erosion rates and changes to runoff generation can greatly augment the amount of sediment released, especially fine-grained particles, nutrients and other constituents that can be delivered to streams and reservoirs affecting water quality in aquatic ecosystems (Ice et al. 2004; Blake et al. 2010; Smith et al. 2011a; Martin 2016; Rust et al. 2019; Robinne et al. 2020).

Understanding soil and sediment process dynamics in fire-affected catchments can support management efforts in facing post-fire soil erosion effects and its downstream impacts. Specifically, the assessment of sediment sources in downstream deposits can support targeted mitigation actions within primary runoff contribution and sediment source areas to reduce the loss of ash and topsoil from hillslopes. Sediment fingerprinting has emerged as a valuable tool in this regard and has been applied in a variety of landscapes and settings (Walling 2013; Owens et al. 2016; Collins et al. 2017, 2020). However, its use in fire-affected landscapes has been relatively limited to applications in Australia (Wilkinson et al. 2009; Smith et al. 2011b), Canada (Owens et al. 2012; Stone et al. 2014) and Spain (Estrany et al. 2016; Garcia-Comendador et al. 2020). While fallout radionuclides (FRNs) have been used to apportion post-fire sources, other tracer properties such as organic compounds (Oros et al. 2002), mineral magnetism (Blake et al. 2006a), colour parameters (Garcia-Comendador et al. 2020) and geochemical elements (Blake et al. 2006b; Owens et al. 2006) have received less attention (Smith et al. 2013). The latter has shown greater potential for source discrimination between fire severities due to wildfire modifications on surface soil geochemistry (Owens et al. 2006; Blake et al. 2006a; Smith et al. 2013) wherein variability in fire severity has been shown to influence the concentration of trace elements in ash and burnt topsoil (Blake et al. 2006b). Herein, important challenges with variability of

geochemical signatures between burnt soil and ash, as well as between burnt and unburnt catchments, have been identified (Smith et al. 2013; Stone et al. 2014).

Plantation forests cover about 131 million ha (3% of the global forest area) and 44% of this area is composed mainly of introduced species. This is particularly relevant in South America where 97% of species are non-native (FAO 2020). Chile has 2.3 million ha of forest plantations, where *Pinus radiata* represent 56% followed by eucalyptus plantations (mainly *Eucalyptus globulus* and *Eucalyptus nitens*) covering 37% of the planted area (INFOR 2020). In Chile, thousands of hectares of forests are lost every year due to the increase in the number of wildfires during dry seasons enhanced by global change, rural depopulation and abandonment of traditional land use practices (Carmona et al. 2012; Urrutia-Jalabert et al. 2018; Gonzalez et al. 2018; McWethy et al. 2018; Gomez-Gonzalez et al. 2019). It has been estimated that fire occurrence in central and south-central Chile has increased by around 50% in the last 40 years (González et al. 2011). Moreover, it has been described that intensive transformation of native forests, shrublands and grasslands into massive exotic pyrophyte forest plantations (e.g. *P. radiata* and *Eucalyptus* spp.) could have a major influence on the magnitude and recurrence of wildfires by changing the fuel structure and flammability of the landscape (Taylor et al. 2017; McWethy et al. 2018; de la Barrera et al. 2018; Mazzorana et al. 2019). Here, the potential of forest plantations to be affected by wildfires requires consideration in terms of the off-site impacts that sediment release from burnt soils areas can have on waterbodies, especially those that are used for drinking water supply (Smith et al. 2011a; Martin 2016).

The increase in the number and severity of wildfire events in Chile (McWethy et al. 2018; de la Barrera et al. 2018), and the potential of forest plantations to be affected (Taylor et al. 2017), means there is an urgent need to evaluate post-fire catchment responses especially within catchments planted with exotic species and hence a higher fire risk. In this context, the aims of this research were (i) to assess dominant sediment sources activated by post-fire rainfall events in a small-forested catchment impacted by a severe wildfire, and (ii) to explore the use of environmental radionuclides combined with elemental geochemistry as tracers to apportion sediment sources within burnt plantation systems.

## 2 Material and methods

### 2.1 Catchment description

Quivolgo catchment is located in “del Maule Region” (Central Chile; Fig. 1). This region is characterised by a temperate and semi-oceanic climate. The main soil type (WRB 1994) is leptosol and haplic luvisol. The annual precipitation ranges

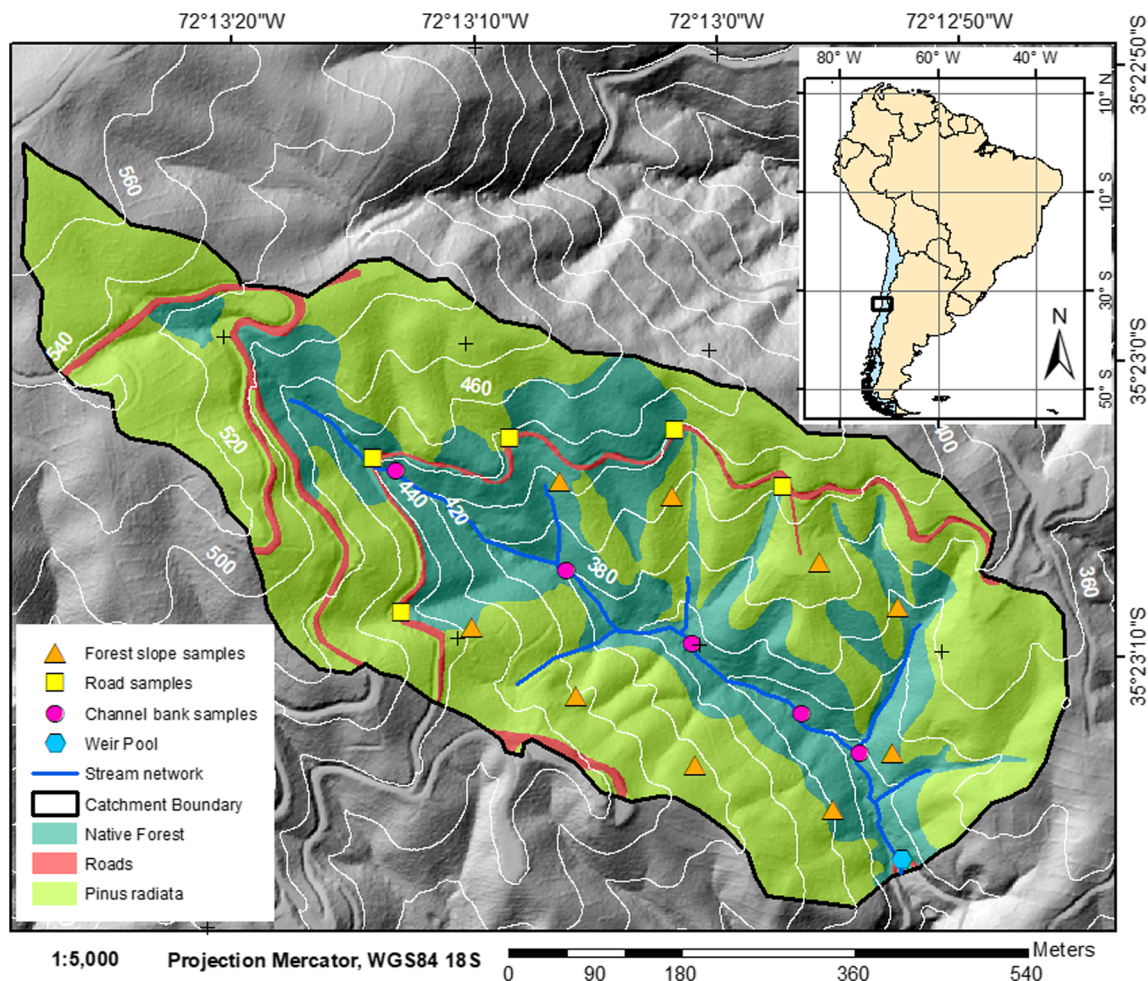


**Fig. 1** Location map of the Quivolgo catchment in Central Chile (35° 23' S, 72° 13' W) showing land uses before wildfire and source and sediment sample locations

are between 860 and 1130 mm (inter-annual coefficient of variation ranges between 0.30 and 0.34%; data not published), and the period of maximum rainfall is from May to September. El Maule region comprises 384,690 ha of land covered with forest plantations, being the third administrative region of Chile with the largest planted area (17% of the total planted land in the country; INFOR 2020). Quivolgo catchment has a total surface area of 40 ha and the stream length is around 0.8 km. The mean altitude is 427 m a.s.l. and the mean slope is 44% (reaching a maximum slope of 121% in some areas). The catchment flow regime is ephemeral. It depends mainly on precipitation, with maximum flow discharge during the winter. During the summer, the mean annual flow decreases markedly to around a 30–60%. The Quivolgo catchment was planted with *Pinus radiata* in 2001 (65.1% of the total surface). Some areas were left intact with native forest species (*Nothofagus glauca*, *Drimis winteri* and *Nothofagus obliqua*; 30.8% of the total catchment area) to provide a riparian buffer strip as a biological corridor to protect watercourses from sediments released during harvesting operations and, at the same time, to keep water physicochemical variables

stabilised (temperature, pH and turbidity). Additionally, forest roads covered 4.2% of the total catchment area at the time of sampling.

During the austral summer of 2017, the central-southern region of Chile suffered one of the biggest forest fires on record. More than 500,000 ha of land were burnt between January 11th and February 18th, where commercial forest plantations were one of the most affected ecosystems (Urrutia-Jalabert et al. 2018; de la Barrera et al. 2018). Furthermore, “El Maule” was the most affected region with 287,027 ha of land being burnt and a total amount of 145,000 ha of commercial forest plantations affected by the fire (de la Barrera et al. 2018). During this wildfire, the entire Quivolgo catchment area was burnt.

## 2.2 Source and sediment sampling

After forest fire, four potential sediment sources were considered for sediment fingerprinting based on previously reported impacts of wildfire on hillslope hydrological processes. Samples from forest hillslopes comprised soil from surface



(first 2 cm of soil surface) and from shallow sub-surface (underneath soil layer of surface soil > 2 cm depth) as defined by the depth of charring. Additionally, surface soil areas deemed to be prone to erosion due to direct connection with the stream network (e.g. channel banks) or exposed to heavy machinery operations within the catchment (e.g. roads) were sampled.

A total of 27 composite source samples were collected within the burnt catchment (3 months after the fire). Forest hillslope composite samples (a mix of five ca. 100 g samples taken from the central point and edges of a 10 × 10 m<sup>2</sup>) were collected to represent the soil surface (0–2 cm, *n* = 9) and the shallow sub-surface material (2–4 cm, *n* = 8) (Fig. 2a). Channel bank soil samples (*n* = 5) were collected next to slopes at the edge of the stream where active erosion was evident (Fig. 2b). Road samples (*n* = 5) were taken from verges, owing to the central trackways being covered by coarse rock aggregate material, and at the opposite side of the forest hillslopes to avoid the influence of sediment that had run-on from the upslope area (Fig. 2c). Source materials were collected using stainless steel spatulas, placed in double plastic bags, labelled accordingly and geo-referenced by GPS.

Bulk sediment samples from the outlet of the Quivolgo catchment were collected from the weir pool, which is a thin plate weir with a 90°-shaped notch coupled with a datalogger pressure sensor (TrueBlue series 555). Weir and data logger installation followed the World Meteorological Organization (WMO) recommendations (WMO 1994), and the sensor was configured to record data every 5 min (Fig. 2d). The weir was emptied and washed after each sampling (to obtain the sediments corresponding to the specific studied periods). Weir samples were collected in May 2017 (weir 1), July 2017 (weir 2) and October 2017 (weir 3). Sediment samples were placed

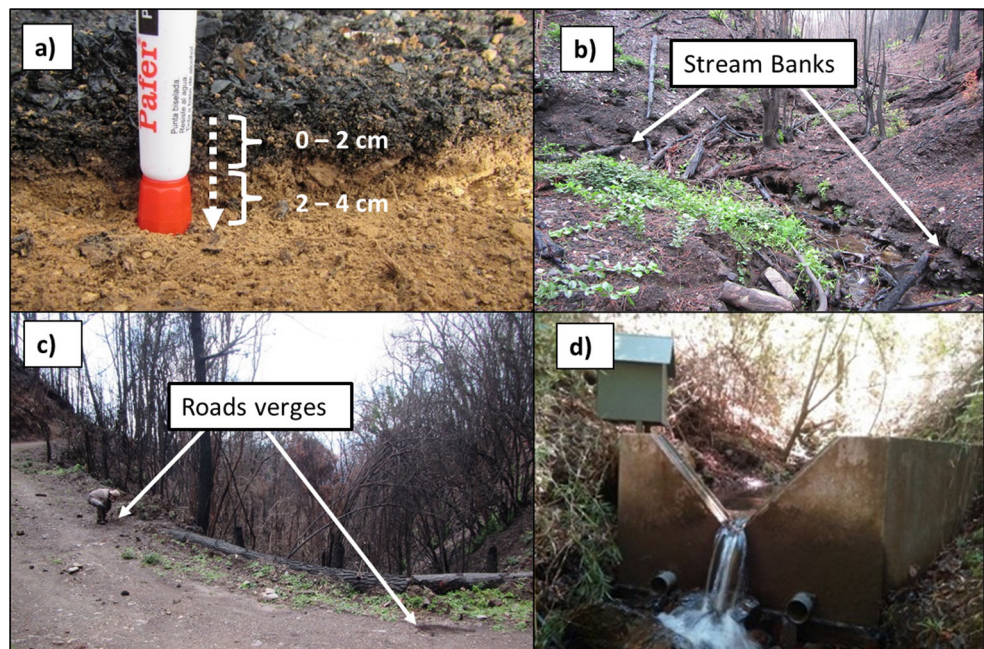
in plastic jars, labelled accordingly and stored for further analysis.

### 2.3 Sample preparation and analysis

The samples were oven-dried at 60°C in aluminium trays covered with Kraft paper (to avoid direct contact of the samples with the tray) and sieved through a 2-mm mesh, obtaining approximately 100 g per sample. Furthermore, samples were sieved to a 63-µm mesh. A 1.0 g sub-sample was taken for particle size analysis (PSA) and the remaining material (~10 g) milled for 20 min at 300 rpm in a Pulverisette 5 planetary ball mill (Fritsch, Germany) using agate milling bowls and balls to achieve homogenous particle size for gamma spectrometry and WD-X-ray fluorescence analyses. Additionally, soil organic matter (% SOM) content was estimated by loss on ignition (LOI). Approximately 5 g subsamples of < 2 mm soil fraction were weighed (in previously cleaned and dried crucibles) and then ignited at 475°C for 3 h in a muffle furnace.

Particle size analysis was performed on the < 63 µm sample material. Prior to particle size analysis by laser granulometry, wet oxidation was carried out to remove organic matter by using 6% H<sub>2</sub>O<sub>2</sub> in a heated water bath (all samples were prepared in triplicate). Particle size analysis was undertaken using a Malvern Mastersizer 2000 (Malvern, UK) with Hydro-G in compliance with ISO 13320. Optimal particle dispersion was achieved using sodium hexametaphosphate (0.2%) in solution and 90 s of ultrasonication during analysis. Pump and stirrer speeds were 2250 and 800 rpm respectively. Each sub-sample was analysed for 30 s using red laser, and this was repeated to produce five data sets for each sub-sample. The software uses an enhanced general model for non-

**Fig. 2** a) Surface and sub-surface soil layers of the burnt catchment. b) Catchment stream/channel banks. c) Road samples taken from the verges. d) V-notched weir pool that receipts sediments transported by the stream channel



spherical particles with an assumed refractive index of 1.53 and initial light adsorption value of 0.01.

Fallout ( $^{137}\text{Cs}$  and  $^{210}\text{Pb}_{\text{ex}}$ ) and geogenic ( $^{226}\text{Ra}$ ,  $^{232}\text{Th}$ ,  $^{238}\text{U}$  and  $^{40}\text{K}$ ) radionuclides were analysed in < 63  $\mu\text{m}$  soil fraction following the methodology described in detail by Appleby (2001). All samples were packed and sealed in gas tight containers. Activity concentrations of the target radionuclides were measured in plastic vials using an ORTEC well detector system (GWL-170-15-S, an N-type detector). The HPGe gamma spectrometry system was built to ultra-low background specification for  $^{210}\text{Pb}$  detection for gamma spectrometry. The instrument was calibrated and operated according to the standard operating procedures contained within the instrument record manual. In brief, the instrument was calibrated using soil material spiked with a certified, traceable mixed radioactive standard 80717-669 (supplied by Eckert & Ziegler Analytics, GA, USA). All calibration relationships were derived using the ORTEC GammaVision software and verified by inter-laboratory comparison tests with materials supplied by the International Atomic Energy Agency (IAEA), in particular the worldwide proficiency test using radioactive moss soil (IAEA-CU-2009-03). The isotopes  $^{210}\text{Pb}$ ,  $^{214}\text{Pb}$  and  $^{137}\text{Cs}$  were determined by their gamma emissions at 46.52, 295.34 (& 351.99) and 661.6 keV, respectively. Total  $^{210}\text{Pb}$  was measured and its unsupported component calculated by the subtraction of the  $^{226}\text{Ra}$  activity, which in turn was measured by the gamma emissions of  $^{214}\text{Pb}$ . To produce activity concentrations, samples were counted for at least 100,000 s. All activity concentration data were decay corrected to the date of sampling. Owing to low activity concentrations and sample mass, 1-sigma counting uncertainties for  $^{137}\text{Cs}$  ranged 12–30% and for  $^{210}\text{Pb}$  ranged 5–18% noting that uncertainties propagated through the mixing model are based on the mean and standard deviation of source group distributions, i.e. the environmental variability and not counting statistics.

Sample analysis for minor and major elements (Na, Mg, Al, Si, P, S, Cl, K, Ca, Ti, Cr, Mn, Fe, Co, Ni, Cu, Zn, Ga, Br, Rb, Sr, Y, Zr, Nb, Ba, Ce and Pb) was undertaken by wavelength-dispersive X-ray fluorescence (WD-XRF) spectrometry. The milled sample material was mixed with a polypropylene wax-binding agent at a ratio of 1:4 (binder:sample), prior to being pressed into sample pellets. Samples were pressed in 40-mm-diameter aluminium sample cups under 150 kN of pressure using a Herzog TP20 manual press. Pellets were analysed for a full suite of elements under vacuum using an Axios max (PANalytical, The Netherlands). The instrument operated an Rh target X-ray tube at 4kW power with sequential detection of elements undertaken with Ar gas flow and scintillation detectors. Measurement conditions were optimised using the PANalytical SuperQ software and the semi-quantitative Omnia analysis application. Instrument drift was assessed following laboratory quality control

procedures using a multi element glass sample (glass monitor C3, Breitlander). Particle size analysis, FRNs and geogenic radionuclides and XRF analyses were performed at the Consolidated Radioisotope Facility (CoRiF) at University of Plymouth, UK.

## 2.4 Statistical analysis and source apportionment

Source and sediment sample value distributions were visualised by using boxplots. Specific comparisons between source groups were statistically tested via a two-sample *t*-test or two-sample Wilcoxon rank sum test (also known as Mann-Whitney *U* test) after checking for test assumptions (e.g. normality and homogeneity of variance).

Tracer selection for source apportionment is a key aspect of the sediment fingerprinting methodology. It has been demonstrated that different tracer selection procedures can lead to substantial variability to the mixing model outputs (Palazon and Navas 2017; Smith et al. 2018). Here a tracer selection procedure was adopted based on the exclusion of apparently non-conservative tracers developed by Smith et al. (2018). Exploratory analysis of sources and mixtures data was undertaken to observe the general geochemical character of the samples. In this case, principal component analysis (PCA) was performed to evaluate source and mixture groupings according to geochemical properties using *FactoMineR* and *factoextra* packages from R (Lê et al. 2008; Kassambara and Fabian 2019). Soil and sediment particle size (via specific surface area, SSA) and soil organic matter (SOM) were tested for significant differences at 95% level of confidence between source groups and between soil and sediment samples after checking test assumptions (e.g. normality and homogeneity of variance). When normality and homogeneity of variance assumptions were met, a two-sample *t*-test (source and mixture groups) and an ANOVA (between source groups) were applied; otherwise, a Wilcoxon rank sum test or Kruskal-Wallis test was carried out. Moreover, the potential non-conservative behaviour in terms of particle sorting effects and/or organic enrichment of tracer concentrations was examined by computing Pearson's correlation with geochemical properties. When assumptions for both Pearson correlation and linear regression were not met (e.g. variables normally distributed and normality of the errors, respectively), a Box-Cox power transformation on tracer values was performed using MASS package in R (Venables and Ripley 2002). When significant correlations ( $p < 0.05$ ) between tracer concentrations and the SSA or SOM were observed, the 95% prediction interval (PI) was computed by simple linear regression to see if sediment mixture values fell within the PI. In this sense, tracers that showed significant correlation with SSA and SOM and where the sediment values fell outside the PI area were discarded from further mixing model analyses. Therefore, tracer properties that remained after correlation/regression analyses were compared between

source and mixture materials through visualisation of source minimum bounding polygons (convex hulls). Where mixtures fell outside the source polygon, an assumption of non-conservative behaviour was made. Consequently, tracers were excluded from further analysis when mixture values lay outside source polygons in most tracer combinations. Finally, source group normality of the remaining tracers was evaluated using Shapiro-Wilks test before the unmixing process.

Sediment source apportionment was carried out using the MixSIAR mixing model package (Stock et al. 2018). MixSIAR is a Bayesian framework that uses tracer data to estimate source probability distributions to a mixture. The fundamental mixing equation followed by MixSIAR and, basically any mixing system, is as follows:

$$Y_j = \sum_k p_k \mu_{jk}^s \quad (1)$$

where the mixture tracer value,  $Y_j$ , for each  $j$  tracer is equal to the sum of the  $k$  source tracer means,  $\mu_{jk}^s$ , multiplied by their proportional contribution to the mixture,  $p_k$  (Stock et al. 2018). The model was run with uninformative priors, using weir pool sampling dates as fixed effects. The error structure was set with the residual error which accounts for unknown sources of variability in weir pool sediment sample apportionment (Parnell et al. 2010). Markov chain Monte Carlo (MCMC) parameters were set as follows: chain length = 3.000.000; burn-in = 1.500.000; thin = 500 and number of chains = 3. Convergence of the model was evaluated using the Gelman-Rubin diagnostic, in which case all variables were below 1.01 (Stock and Semmens 2018). All results are provided as the mean and standard deviations from the posterior distributions obtained by MixSIAR. The matrix plot of correlation between global posterior source probability distributions was used to evaluate the quality of source discrimination. Finally, source apportionment results were compared with results obtained using tracers that passed the classical tracer selection procedure (e.g. range test, Kruskal-Wallis test and discrimination function analysis, DFA) first introduced by Collins and Walling (2002). The above described methodology was applied via FingerPro package in R (Lizaga et al. 2020). All statistics and unmixing process were done in R (R Core Team 2018) via RStudio interface (RStudio Team 2015).

## 3 Results

### 3.1 Catchment hydrological response to wildfire

Accumulated monthly precipitation in the Quivolgo catchment is focussed on winter months (from May to September) accounting for between 200 and 250 mm (Fig. 3). During the study period, pluviometric conditions were

similar except for 2016, where precipitation decreased by 46% compared to the mean rainfall during 2014 and 2015. Also, precipitation recorded in 2017 was notably higher compared to previous years (Fig. 3). Flow discharge at the weir was sensitive to rainfall during each season and the minimum flow was registered before the wildfire event. After the fire, discharge ( $\text{m}^3 \text{s}^{-1}$ ) increased almost twofold compared to pre-fire streamflow conditions (Fig. 3).

### 3.2 Radionuclide activity and elemental concentration of tracers after wildfire

An increase of 1.5 and 4.5 times in the activity concentration of  $^{137}\text{Cs}$  and  $^{210}\text{Pb}_{\text{ex}}$ , respectively, was observed in burnt materials of surface layers compared to soil surface values from hillslope samples of a previous study in the same catchment before wildfire (Table 1; data not published). In this sense,  $^{137}\text{Cs}$  and  $^{210}\text{Pb}_{\text{ex}}$  mean activity concentrations ( $\text{Bq kg}^{-1}$ ) in surface soil samples of the burnt catchment were significantly higher than surface soil samples before fire ( $^{137}\text{Cs}$  = one-sided two-sample  $t$ -test,  $t(19) = 3.2834$ ,  $p < 0.01$ ;  $^{210}\text{Pb}_{\text{ex}}$  = Welch one-sided  $t$ -test,  $t(7.58) = 5.57$ ,  $p < 0.0001$ ).

Moreover,  $^{210}\text{Pb}_{\text{ex}}$  sub-surface values were significantly lower than surface values after wildfire (Welch one-sided  $t$ -test,  $t(9.07) = -3.217$ ,  $p < 0.01$ ; see  $^{210}\text{Pb}_{\text{ex}}$  value distribution at Fig. 4), whereas  $^{137}\text{Cs}$  did not show significant differences between these two sources (one-sided two-sample  $t$ -test,  $t(14) = -0.543$ ,  $p > 0.05$ ). It is noteworthy that  $^{210}\text{Pb}_{\text{ex}}$  mean activity for surface samples ( $77 \pm 30 \text{ Bq kg}^{-1}$ ) was almost two times higher than sub-surface samples ( $41 \pm 12 \text{ Bq kg}^{-1}$ ; see Table 1). Furthermore,  $^{137}\text{Cs}$  values for channel bank samples after wildfire were not statistically different to surface samples (Welch two-sided  $t$ -test,  $t(7.01) = -0.20$ ,  $p > 0.05$ ), where mean activities were similar:  $5.8 \pm 0.0 \text{ Bq kg}^{-1}$  and  $5.9 \pm 2.1 \text{ Bq kg}^{-1}$ , respectively (see Supplementary Table 1). However, differences in  $^{210}\text{Pb}_{\text{ex}}$  values between these two sources were significant (Welch two-sided  $t$ -test,  $t(8.21) = -3.43$ ,  $p < 0.05$ ). Additionally, significant differences between channel banks and sub-surface samples were not observed for either tracers ( $^{137}\text{Cs}$ : Welch two-sided  $t$ -test,  $t(7.02) = 0.616$ ,  $p > 0.05$ ;  $^{210}\text{Pb}_{\text{ex}}$ : two-sided two-sample  $t$ -test,  $t(12) = -0.2411$ ,  $p > 0.05$ ).

Elemental concentrations of Na, Mg, Al, P, K, Ca, Mn, Fe, Co, Zn, Sr and Ba in surface material were significantly higher than sub-surface (Na, Mg, Al, P, K, Mn, Fe, Co, Sr and Ba: one-sided two-sample  $t$ -test,  $t(15)$  less than  $-1.88$ ,  $p < 0.05$ ; Ca and Zn: one-sided two-sample Wilcoxon rank sum test,  $W > 6$ ,  $p < 0.05$ ; see for example, Mg, K and Mn value distribution at Fig. 4). The opposite was true for Cl which showed a mean concentration value for surface soil samples significantly lower than sub-surface (one-sided two-sample  $t$ -test,  $t(15) = 2.25$ ,  $p < 0.05$ ). Additionally, Na, Mg, P, K, Zn, Rb, Sr and Pb showed significant differences between channel bank and



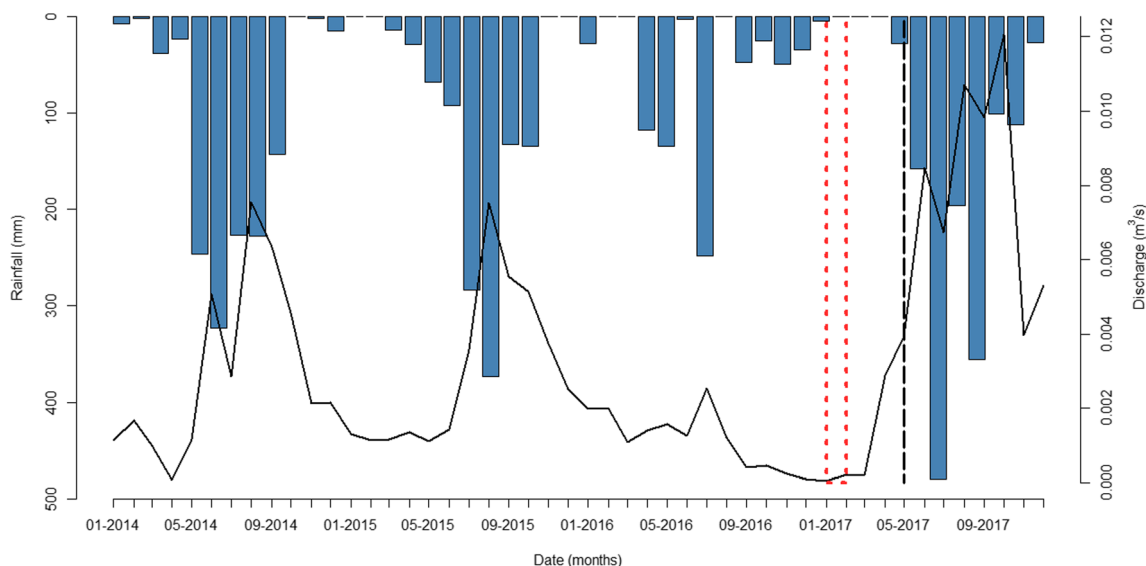


**Fig. 3** Accumulated monthly rainfall (mm) and flow discharge ( $\text{m}^3 \text{s}^{-1}$ ) at weir between 2014 and 2017 in Quivolgo catchment. The period when the wildfire occurred is delimited with a red-dotted line, and the source

sampling campaign is indicated by a black vertical dashed line. Note that the rainy period starts in April–May and ends in October (southern hemisphere)

sub-surface sample values (Na, K, Zn, Rb, Sr and Pb: two-sided two-sample  $t$ -test,  $t(12) > 2.4$ ,  $p < 0.05$ ; Mg: Welch two-sided  $t$ -test,  $t(10.2) = 5.53$ ,  $p < 0.001$ ; P: Wilcoxon rank sum test,  $W = 45$ ,  $p < 0.001$ ), while Al, Si, S, Cl, Ca, Ti, Cr, Mn, Fe, Co, Ni, Cu, Ga, Y, Zr, Nb, Ba and Ce did not present significant differences between these source values (Si, S, Cl, Ti, Cr, Mn, Ni and Zr: two-sided two-sample  $t$ -test,  $t(12) < 2.07$ ,  $p > 0.05$ ; Fe, Co and Y: Welch two-sided  $t$ -test,  $t(\text{Fe}: 4.4; \text{Co}: 3.4 \text{ and } \text{Y}: 10.2) = 1.06, 1.49 \text{ and } 0.52$  for Fe, Co and Y, respectively,  $p > 0.05$ ; Al, Ca, Cu, Ga and Nb: Wilcoxon rank sum test,  $W < 21$ ,  $p > 0.05$ ; see for example, Ti, Mn and Zr value distribution at Fig. 4).

### 3.3 Tracer selection procedure

The SSA of sampled soil materials from the Quivolgo catchment presented significant differences in their distribution (Kruskal-Wallis test,  $H = 19.6$ ,  $p < 0.001$ ; see SSA distribution at Fig. 5). For example, sub-surface materials

presented SSA values significantly lower than those of surface (Wilcoxon rank sum test,  $W = 10$ ,  $p < 0.01$ ). Additionally, RO samples showed the lowest mean of SSA among sources ( $0.17 \pm 0.03 \text{ m}^2 \text{ g}^{-1}$ ; Supplementary Table 1). Therefore, source and sediment sample groups showed significant differences in SSA values (Wilcoxon rank sum test,  $W = 60$ ,  $p < 0.05$ ).

In contrast to SSA, % SOM did not present significant differences between source and sediment samples (two-sided two-sample  $t$ -test,  $t(34) = -0.57$ ,  $p > 0.05$ ). Differences between source samples, however, were significant (one-way ANOVA,  $F(3, 23) = 12.11$ ,  $p < 0.001$ ; see % SOM distribution at Fig. 5). Additionally, road samples showed the lowest mean organic content ( $7.0 \pm 2.2$ , see Supplementary Table 1), whereas the highest mean in soil organic matter was observed in sub-surface samples ( $16.2 \pm 3.2$ , see Table 1 and Supplementary Table 1). Furthermore, % SOM between surface and channel banks were similar ( $12.2 \pm 2.9$  and  $13.1 \pm 2.0$ , respectively. See Supplementary Table 1).

**Table 1** Percentage of soil organic matter and activity concentration ( $\text{Bq kg}^{-1}$ ) of  $^{137}\text{Cs}$  and  $^{210}\text{Pb}_{\text{ex}}$  of hillslope surface soil samples from pre-fire and post-fire situation in the Quivolgo catchment. Soil samples from hillslopes were collected from the topsoil first centimetre in 2014 (data not published)

|                           | SOM (%) |      | $^{137}\text{Cs}$ ( $\text{Bq kg}^{-1}$ ) |     | $^{210}\text{Pb}_{\text{ex}}$ ( $\text{Bq kg}^{-1}$ ) |      | <i>n</i> |
|---------------------------|---------|------|---|-----|---|------|----------|
|                           | Mean    | SD   | Mean                                      | SD  | Mean  | SD   |          |
| Pre-fire                  |         |      |   |     |   |      |          |
| Forest slopes (0–1 cm)    | 25.1    | 10.1 | 3.5                                       | 1.2 | 16.5  | 7.0  | 13       |
| Post-fire                 |         |      |   |     |   |      |          |
| Surface soil (0–2 cm)     | 12.2    | 2.9  | 5.9                                       | 2.1 | 77.4  | 30.0 | 9        |
| Sub-surface soil (2–4 cm) | 16.2    | 3.2  | 5.4                                       | 1.7 | 40.8  | 12.3 | 8        |

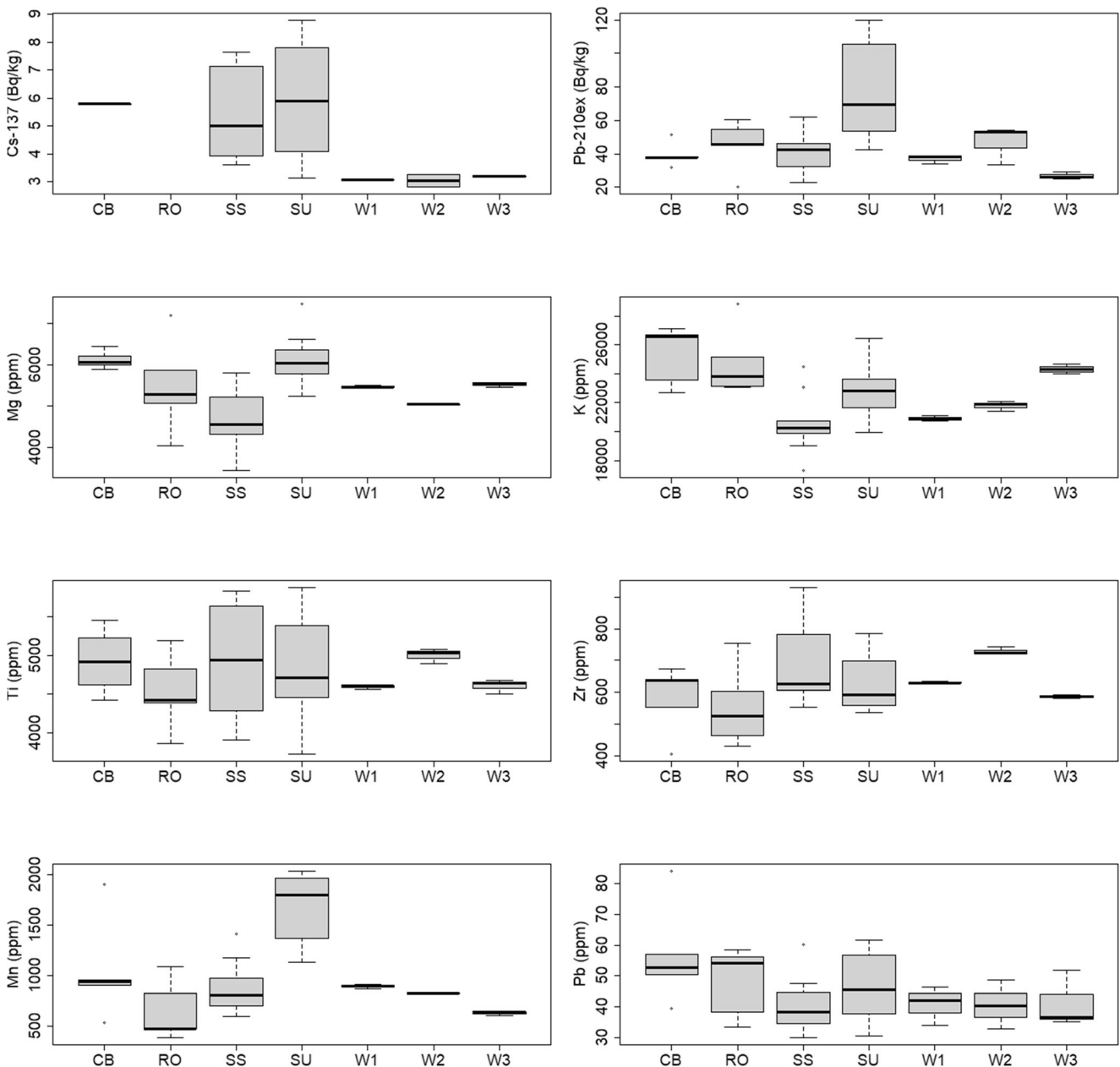


**Fig. 4** Boxplots of soil and sediment sample value distribution of FRNs ( $^{137}\text{Cs}$  and  $^{210}\text{Pb}_{\text{ex}}$ ) and some geochemical elements (i.e. Mg, K, Ti, Zr, Mn and Pb).  $^{137}\text{Cs}$  activity in road samples were all below minimum

detectable activity (< MDA). CB: Channel Banks, RO: Roads, SS: Sub-surface, SU: Surface, W1: Weir 1, W2: Weir 2, W3: Weir 3

Due to the above differences between source groups and sediment mixtures, SOM and SSA linear relationships with tracer properties were evaluated. In the present study, tracers that showed significant correlation ( $p < 0.05$ ) between SSA and elemental concentrations were  $^{226}\text{Ra}$ , Si, P, S, Cl, Ca, Mn, Cu, Zn, Sr and Ba (see Supplementary Table 2). Nevertheless, the 95% linear regression PI (Fig. 6) showed that only S, Cl and Ca mixture values plotted outside PI and hence were considered to be exhibiting a non-conservative behaviour relative to sediment samples (Smith et al. 2018). These three tracers were consequently removed from further analysis.

Soil organic matter presented significant correlations ( $p < 0.05$ ) with Si, S, Cl, K, Ca and Nb (Supplementary Table 2) but only S and Cl mixture values fitted outside the PI of the combined sources (Fig. 7). It is noteworthy that these tracers showed a highly significant relationship with SOM ( $p < 0.001$ ) and the strong positive association between S and Cl with SOM ( $r = 0.8$ , see Supplementary Table 2) suggests an enrichment of these tracers with increased soil organic content. Therefore, S and Cl interaction with SOM demonstrated their inability to be used as sediment tracers in catchments



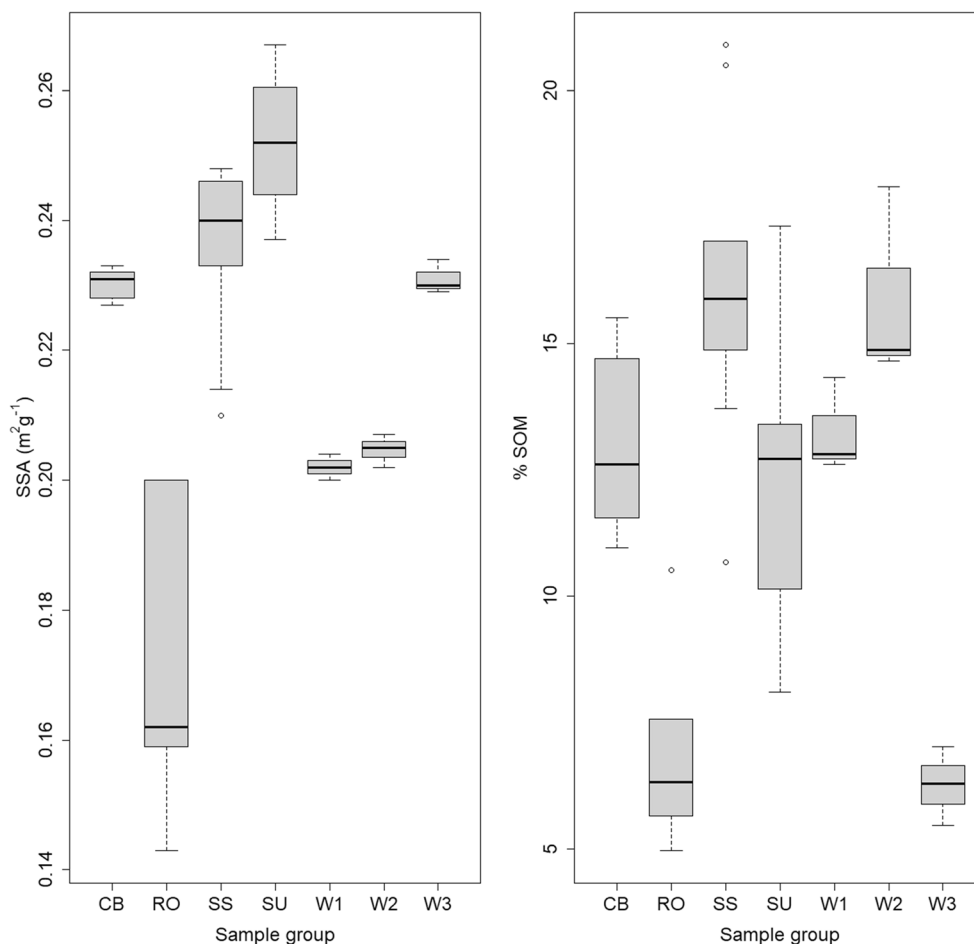


**Fig. 5** Boxplots of SSA ( $\text{m}^2 \text{g}^{-1}$ ) and SOM (% loss-on-ignition) of sample distribution for source soils and weir pool sediment samples ( $< 63 \mu\text{m}$  fraction). CB: Channel Banks, RO: Roads, SS: Sub-surface, SU: Surface, W1: Weir 1, W2: Weir 2, W3: Weir 3

affected by wildfire and consequently, they were removed for sediment apportionment calculations.

The source convex hull of the remaining tracers (28) showed that for ten tracers, sediment mixtures plotted inside the bounding polygon in most of tracer combinations (half number of tracers + 1) (see Supplementary Table 3). Following this process,  $^{210}\text{Pb}_{\text{ex}}$ , Mg, Si, K, Ti, Mn, Y, Zr, Nb and Pb were selected as good performers and they were evaluated to be included in subsequent source apportionment calculations. The remaining tracers (e.g.  $^{226}\text{Ra}$ ,  $^{232}\text{Th}$ ,  $^{238}\text{U}$ ,  $^{40}\text{K}$ , Na, Al, P, Cr, Fe, Co, Ni, Cu, Ga, Rb, Sr, Ba and Ce) were excluded. In addition, we noticed that extreme outliers affected the source polygon area considerably which could lead to the potentially erroneous inclusion of sediment samples within the polygon boundary. When outliers were one or more orders of magnitude greater than the mean source tracer value distribution, they were removed only from the convex hull computation. An example of convex hull polygon criteria can be found in the Supplementary Figure 1.

In addition, the normality of source group tracers was evaluated. Tracers that fitted normal distribution were Mg, Si, K, Ti, Y, Zr and Nb ( $W > 0.93$ ,  $p > 0.05$ ) while  $^{210}\text{Pb}_{\text{ex}}$ , Mn and Pb did

not ( $W < 0.92$ ,  $p < 0.05$ ). Nevertheless, these tracers were kept in further steps owing to relaxation of the source normality assumption in MixSIAR, supported by Smith et al. (2018) who showed that the removal of tracers on the basis of non-normality led to a decrease in mixing model accuracy using synthetic mixtures.

Additionally, principal component analysis (PCA) of soil and sediment samples was undertaken after the tracer selection procedure to explore the geochemical behaviour of source observations (Fig. 8). PCA of remaining tracers led to a high dispersion of source observations (Fig. 8), which can be seen in the low value of explained variance by the first principal component (33% of explained variance). Confidence source ellipses at 95% level showed a clear distinction between the surface and sub-surface sample groupings mainly explained by the influence of  $^{210}\text{Pb}_{\text{ex}}$ , Mn and Pb tracer values. Also, separation between sub-surface and channel bank groupings is noteworthy. However, overlap between road samples and other source sample confidence ellipses were observed which evidence low discriminatory capacity of tracers between some materials. Additionally, sediment sample confidence ellipses of weir 1 and weir 2 plotted inside of sub-surface ellipse while weir 3 plotted inside the road source ellipse.

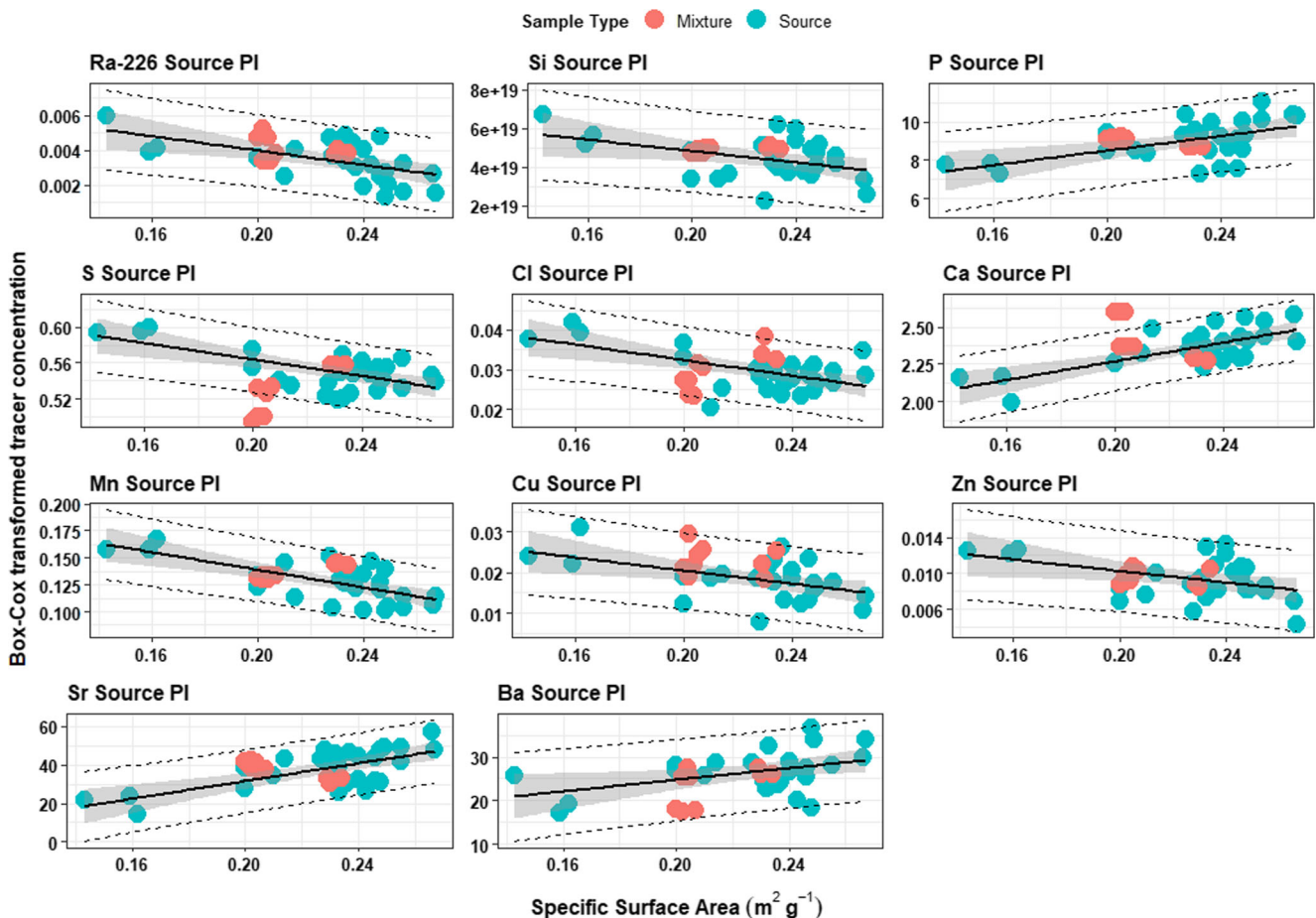


**Fig. 6** The 95% prediction intervals (dashed lines) and 95% confidence interval (shaded area) of source linear regression between the specific surface area ( $\text{m}^2 \text{g}^{-1}$ ) and Box-Cox transformed tracer concentration

### 3.4 Post-fire sediment source contributions and tracer selection method comparison

According to mixing model outputs, the main sources of sediment that accumulated in the weir after the wildfire (from December 2016 until May 2017) were shallow sub-surface soil followed by forest roads i.e.  $55 \pm 11$  and  $30 \pm 11\%$ , respectively (summary statistics can be found in Supplementary Table 4). During June and July 2017, weir sediment samples had sub-surface contributions in excess of  $78 \pm 10\%$ . Between August and October 2017, roads were the dominant sediment source contributing  $71 \pm 14\%$  with a notably lower proportion of sub-surface ( $19 \pm 10\%$ ). Surface soil and channel bank apportionment were negligible during the whole study period ( $< 10\%$ , Fig. 9). In addition, important correlation was observed between roads and sub-surface global posterior distributions ( $r = -0.71$ ), whereas association between remaining source posterior distributions was weak ( $r$  less than  $-0.36$ , see Supplementary Figure 2).

In comparison, the classical tracer selection procedure resulted in five tracers suitable for apportionment calculations, which were selected on the basis of maximised discrimination

among sources. Tracers that passed the range test, Kruskal-Wallis test and DFA test were  $^{226}\text{Ra}$ , P, Cl, K and Sr. It is important to highlight that K was the only tracer that was selected in both tracer selection methods. In addition, Cl was included in this set of tracers even when it was considered non-conservative since it had strong association with SSA and SOM and plotted sediment samples outside PI ( $r = -0.6$ ,  $r = 0.8$  and Fig. 6, Fig. 7, respectively; also see Supplementary Table 2).

Sediment source apportionment with classical tracer selection did not show notable difference in results from the more holistic approach in terms of dominant sources. The same dominant sediment sources i.e. sub-surface in the first two periods and roads in the last period were identified (Fig. 10) although differences in the estimated percent of contribution were seen. For example, at weir 2 (June–July), sub-surface contribution accounted for  $40 \pm 14\%$  (see Supplementary Table 5) and, at weir 3 (August–October), road contribution was  $56 \pm 15\%$ . In both cases, classical statistics-driven tracer selection procedure resulted in the reduction of the apportionment from these sources compared to the more holistic and inclusive tracer selection applied in this study. Conversely,

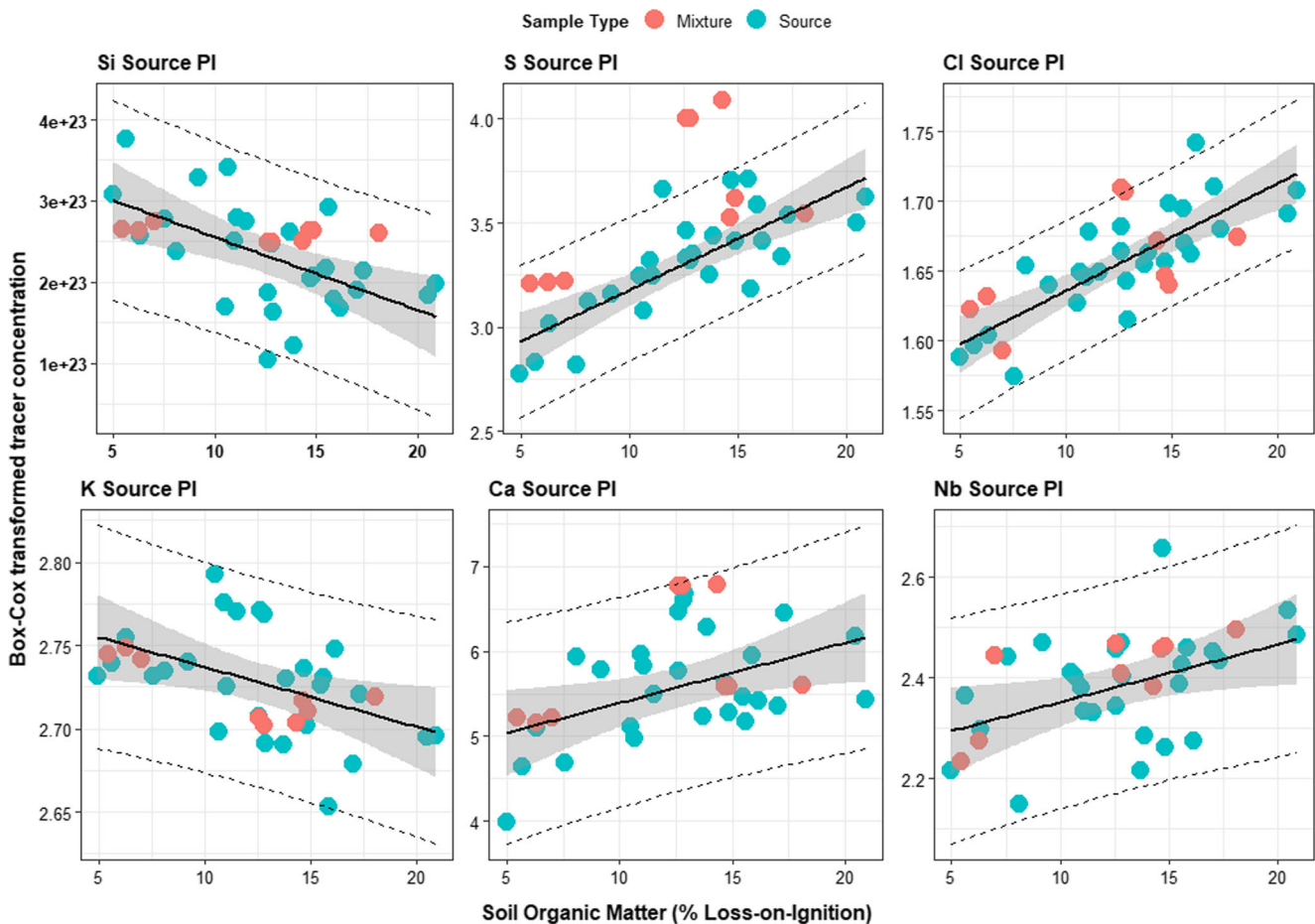


**Fig. 7** The 95% prediction intervals (dashed lines) and 95% confidence interval (shaded area) of source linear regression between the soil organic matter (% loss-on-ignition) and Box-Cox transformed tracer concentration

channel bank contribution increased almost 15%, whereas surface soil apportionment was negligible at these three periods. Furthermore, it is noteworthy that the classic tracer selection procedure resulted in wider posterior distributions for the main sources in the periods evaluated compared with the method applied in this study (see Fig. 10). For instance, credible intervals (CIs) of sub-surface probability distribution in weir 1 and weir 2 ranged between 8–66% and 10–70% respectively compared to 32–77% and 55–95% for weirs 1 and 2, respectively. The same is true for road sources at weir 3, where posterior probability CI ranged from 24 to 84% with classic tracer selection compared to the selection method applied in this study, whose CIs ranged from 41 to 83%.

## 4 Discussion

### 4.1 Tracer distribution values in soil samples

The increase of FRN activity in surface of burnt soil compared with surface soil values before wildfire was in line with other studies which have found that wildfires enhance FRN

concentration due to the combustion of organic matter (e.g. leaf litter and humic materials) (Johansen et al. 2003; Wilkinson et al. 2009; Owens et al. 2012; Estrany et al. 2016). Fallout  $^{210}\text{Pb}_{\text{ex}}$  would have been deposited on pine needle duff layer and on native tree canopy prior to the fire and when they were reduced to ash, the  $^{210}\text{Pb}_{\text{ex}}$  was therefore concentrated on the surface (Owens et al. 2012; Smith et al. 2013). On the other hand, large spatial variability was observed for FRNs in surficial samples after forest fire (see  $^{137}\text{Cs}$  and  $^{210}\text{Pb}_{\text{ex}}$  boxplots at Fig. 4). In surface material, the within-source variability of both  $^{137}\text{Cs}$  and  $^{210}\text{Pb}_{\text{ex}}$  may be due to the following reasons: (1) spatial variation in the intensity of the wildfire and the degree of combustion of organic matter, (2) variations in ash deposition and (3) the extent of ash infiltration into surface soil layers (Owens et al. 2012; Estrany et al. 2016). The latter is attributed to a low intensity rain that occurred a few days before sampling that may have caused the incorporation of part of the ash deposits into the surface soil layer through infiltration leading to sealing of pores and macropores.

The similarity in terms of FRN composition between channel banks and sub-surface samples can be attributed to the sample depth in the soil profile, where sub-surface soil corresponds to



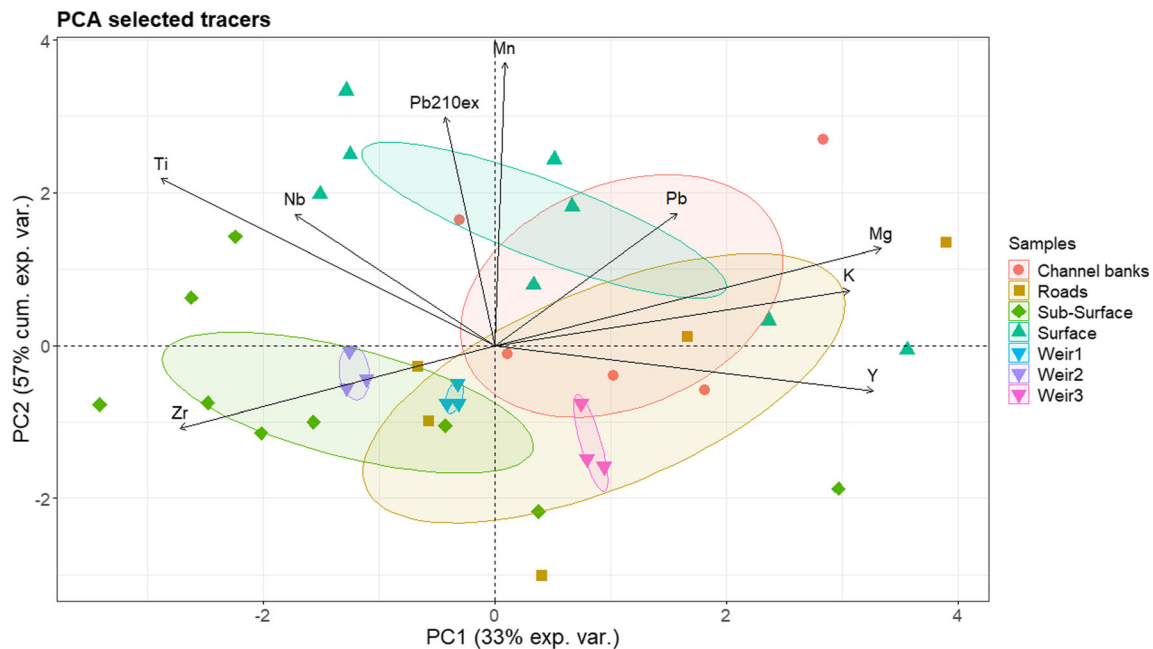


**Fig. 8** Principal component analysis of tracers selected by the criteria applied for burnt catchment sediment apportionment. Ellipses represent 95% confidence level of group distributions in the hyper-space. In the case of missing values, the mean tracer value was included for visualisation purposes

the 2–4 cm soil layer and stream channel incisions are relatively shallow (as can be seen at Fig. 2b). Furthermore, the discrepancy between surface and sub-surface statistical differences in  $^{137}\text{Cs}$  and  $^{210}\text{Pb}_{\text{ex}}$  values can be associated with the tendency for  $^{210}\text{Pb}_{\text{ex}}$  to present higher concentration in the ash due to its continuous production, residence in the surface litter and delivery, whereas  $^{137}\text{Cs}$  tends to have greater association with deeper soil material following the cessation of  $^{137}\text{Cs}$  fallout (Blake et al. 2009b; Owens et al. 2012; Smith et al. 2013). Additionally, the absence of  $^{137}\text{Cs}$  activity in forest road samples is a consequence of surface soil being removed during road construction, in contrast to  $^{210}\text{Pb}_{\text{ex}}$ , which has been deposited continuously from the atmosphere.

The increase in concentration of Na, Mg, Al, P, K, Ca, Mn, Fe, Co, Zn, Sr and Ba in surface soil samples can be attributed to the mineralisation of soil organic matter with further inputs from canopy due to combustion (Certini 2005; Owens et al. 2006; Smith et al. 2013). On the contrary, decrease in Cl concentration may be due to volatilisation from surface layers associated with soil heating or leaching to sub-surface layers (Owens et al. 2006; Smith et al. 2013). On the other hand, the similarities in element composition between sub-surface and channel banks (e.g. Al, Si, S, Cl, Ca, Ti, Cr, Mn, Fe, Co, Ni, Cu, Ga, Y, Zr, Nb, Ba and Ce) support that channel banks present sub-surface material.

## 4.2 Tracer selection

It is important to give consideration to the potential influence of particle size selectivity in erosion processes e.g. where fine particles have greater potential to be transported

and may become geochemically enriched in certain properties (Smith and Blake 2014; Laceby et al. 2017). SSA can control some elemental concentration where interactions are due to adsorption or where there is a compositional control on size fraction e.g. silica and sand particles. While relationships vary in complexity, it has been shown that below  $1.0 \text{ m}^2 \text{ g}^{-1}$ , the relationship between these interactions is approximately linear (Smith and Blake 2014; Laceby et al. 2017). The impacts of wildfire on hydrological and morphological processes are commonly associated with a change in soil aggregate stability and enhanced or decreased water repellency, which could have implications for infiltration, overland flow and rain splash detachment of soil particles (Shakesby and Doerr 2006; Blake et al. 2007). Furthermore, it has been demonstrated that soil burning can significantly reduce the clay content with corresponding increase in sand-sized particles (Dyrness and Youngberg 1957) implying aggregation of fine particles into robust coarser composite particles. Conversely, some other studies have shown no significant change in soil aggregate size distribution following a burning episode (Garcia-Corona et al. 2004). In this sense, surface materials presented SSA values significantly higher than those of sub-surface (see Fig. 5) indicating that sub-surface soil was coarser than surface soil whose structure and aggregate stability could have been affected by wildfire (Blake et al. 2009a), mainly by the influence of ash particles that may have been incorporated into the soil surface. Also, it is important to highlight that roads presented the lowest SSA mean, indicating that road material was composed of coarser particles than other soils within the catchment.

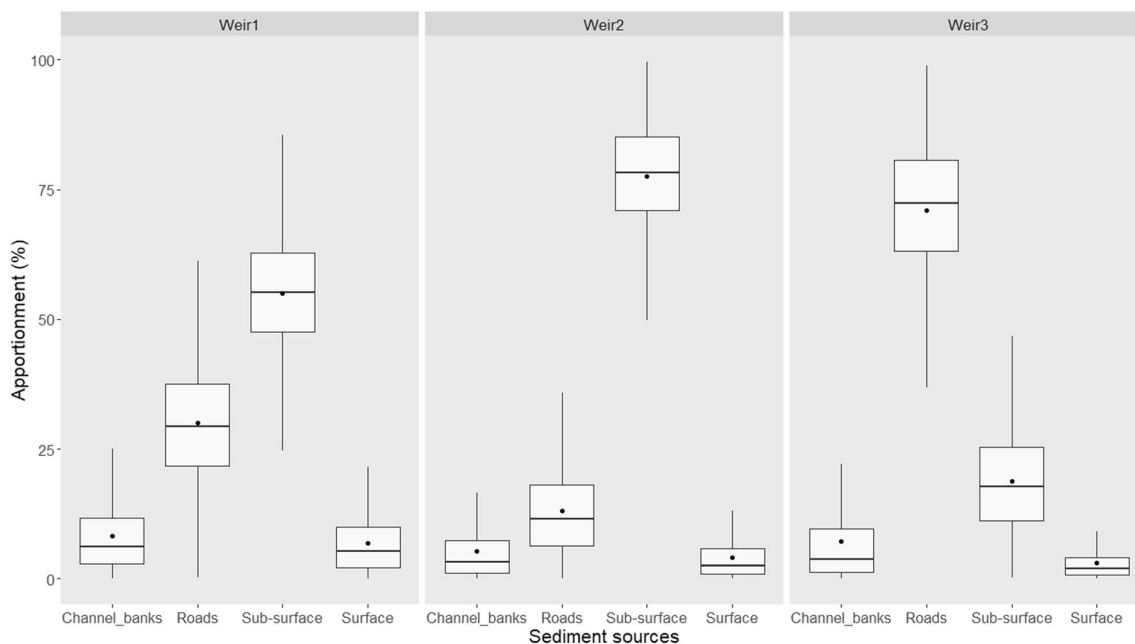


**Fig. 9** Boxplots of posterior source probability distributions (%) for post-fire sediment samples during May (weir 1), July (weir 2) and October (weir 3) 2017

Burning will substantially modify SOM properties (Ice et al. 2004; Certini 2005) thereby affecting tracer concentration properties (e.g. enrichment of trace elements in ash). In some prior studies, researchers have incorporated correction factors to deal with this issue, while other authors have decided to leave concentration properties without modification to avoid over-correction (Smith et al. 2011b). Some other studies have raised concern about using correction factors (Koiter

et al. 2018), while Smith and Blake (2014) found that applying combined SSA and total organic content correction completely altered source tracer content (e.g.  $^{210}\text{Pb}_{\text{ex}}$  activity). In the Quivolgo catchment, surface SOM decreased twofold compared to unburnt surface SOM (see Table 1), and it was also lower compared to sub-surface samples after wildfire (see Fig. 5), suggesting a depletion in surface SOM caused by burning. Wildfire should not affect or otherwise have a minor

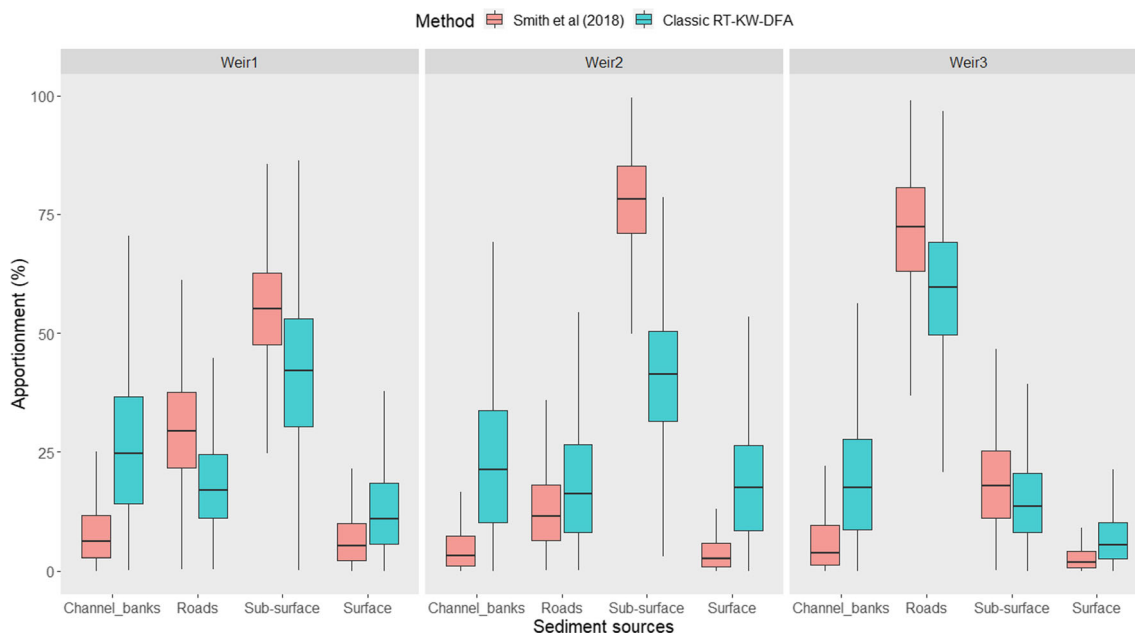


**Fig. 10** Boxplots for posterior source probability distributions (%) obtained from the two tracer selection methods: classical range test, Kruskal-Wallis test and discriminant function analysis and the method

described by Smith et al. (2018). RT, KW and DFA refer to range test, Kruskal-Wallis test and discriminant function analysis, respectively

impact on road material organic content. Therefore, low values are attributed to the intrinsic composition of forest road cover (mainly influenced by the input of fallen pine needles and branches).

The tracers that passed the selection process were  $^{210}\text{Pb}_{\text{ex}}$ , Mg, Si, K, Ti, Mn, Y, Zr, Nb and Pb. These fingerprinting properties were selected based on weak and non-significant linear relationship between tracer concentrations and SSA and SOM, thereby negligible alteration of tracer properties due to enrichment or depletion, and conservative behaviour supported by the inclusion of sediment samples within source convex hull boundaries for all tracer combinations. Furthermore, Si, Ti, Y and Zr have been described as conservative due to their preference to be matrix-bound to sediments (Collins et al. 2020) and  $^{210}\text{Pb}_{\text{ex}}$  have enough half-life to consider it as conservative in contemporary sediment dynamics (Koiter et al. 2013). In contrast, the use of K and Mg as tracers has been challenged in sediment fingerprinting investigations due to its water solubility potential (Kraushaar et al. 2015). Nevertheless, these two tracers were kept in mixing modelling calculations due to their discriminatory potential between surface and sub-surface sources in a forest fire context (Blake et al. 2006b; Owens et al. 2006; Smith et al. 2013).

Principal component analysis of selected tracers showed an important overlap between surface and channel bank ellipses. This could be attributed to the influence of surface material inputs into some parts of stream banks due to ash export downslope where soil colour denotes the influence of burnt surface in some areas (see Fig. 2b). It is important to highlight the influence of  $^{210}\text{Pb}_{\text{ex}}$ , Mn and Pb elemental concentration on these sources (see Fig. 4 and Fig. 8). Moreover, overlap between roads and sub-surface ellipses was also observed, indicating the similar geochemistry between these two sources (mainly explained by the influence of Zr and Y concentrations).

### 4.3 Post-fire sediment source apportionment and its implications

#### 4.3.1 Catchment hydrological response to wildfire

The increase in streamflow after fire (Fig. 3) is not only attributed to rainfall, but also linked to reduced infiltration that may be compounded by soil water repellency and reduction in evapotranspiration (Ice et al. 2004; Certini 2005; Shakesby and Doerr 2006) and also the loss of rainfall interception by the canopy (up to 65% reduction in the rainfall interception according to Williams et al. 2019). These changes may have generated an increase in runoff and subsequently an increase in flow discharge (Fig. 3).

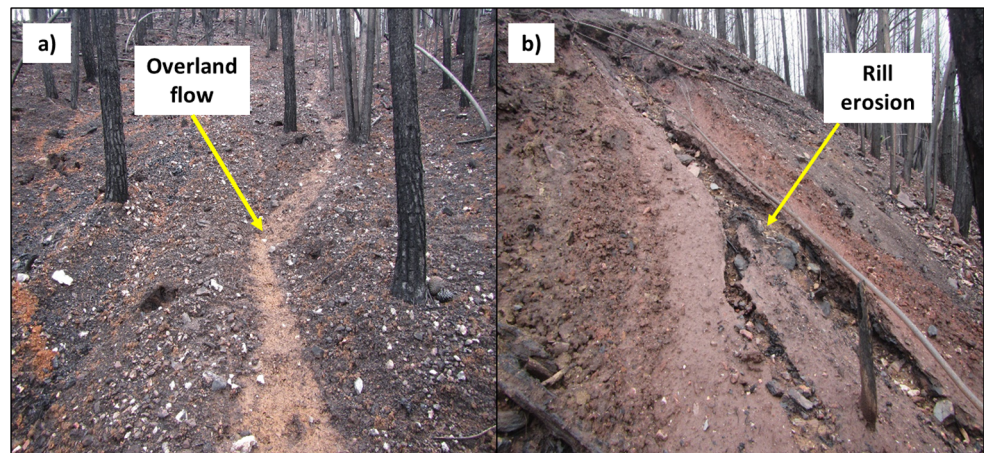
#### 4.3.2 Shifts in post-fire sediment sources

The dominance of shallow sub-surface material as a sediment source during the first two periods can be attributed to rill erosion that took place in the catchment hillslopes after the wildfire due to convergence of overland flow from the first rainfall (as seen in Fig. 11 a-b). The generation of surface runoff and rill erosion mechanisms in burnt catchments has been reported because of reduced infiltration capacity due to clogging of pore space by ash and/or soil water repellency distribution in the soil profile during wildfire (Ice et al. 2004; Shakesby and Doerr 2006). Under the “extreme” soil water repellency model, rainfall saturates a wettable burnt surface soil layer which slides downslope over an enhanced water-repellent sub-surface carrying substantial quantities of ashes and sediments (e.g. surface soil in this study) (DeBano 2000; Shakesby and Doerr 2006; Smith et al. 2013). While overland flow processes were clearly enhanced in the Quivolgo catchment due to the rainfall received during winter months (maximum rainfall peak reached during July 2017; see Fig. 3), a post-fire water repellency-driven sheet-wash/mass wasting model does not support the observation of dominant sub-surface soil release by rill erosion (2–4 cm). Here, it seems more likely that the low-infiltration capacity of ash-covered surface has remained relatively cohesive and the overland flow has only achieved sufficient competence to entrain surficial material along flow convergence lines which are rapidly incised leading to dominant sub-surface soil erosion through rilling.

The uppermost surface material (0–2 cm) was not an important sediment source in the three periods evaluated (Fig. 9). The burnt surface material was observed in inter-rill zones in situ during the sampling campaign (May 2017, 3 months after the wildfire finished, Fig. 3a) when the rainy period had recently started. This finding contrasts with other studies that observed burnt hillslope surface as the major sediment source in catchments affected by wildfires (Blake et al. 2009b; Wilkinson et al. 2009; Smith et al. 2011b) where arguably soil water repellency dynamics are notably enhanced due to local vegetation type (e.g. eucalyptus). Furthermore, post-fire erosion from channel banks was not an important sediment source in the three periods evaluated, which contrasts with observations by Owens et al. (2012) who attributed that sub-surface/channel bank erosions were key factors in sediment production in forested catchments after fire. This discrepancy may be due to the following factors: (i) buffer zone stabilisation due to riparian vegetation before the fire specially at the first sampling period, in contrast to Owens et al. (2012) where tree death led to channel-side tree falls and loss of root strength, and (ii) water level and streamflow power during the rainy periods was not sufficient to erode banks, although



**Fig. 11** Steep slopes in Quivolgo catchment where **a**) overland flow and **b**) consequent rill erosion are the main drivers of sediment transport towards the stream channel



differences in study design and source sampling should be considered.

Forest roads have been reported as a major sediment source in commercial forest catchments without wildfire impacts (Motha et al. 2003; Schuller et al. 2013; Brandt et al. 2018; Bravo-Linares et al. 2020). Additionally, a study was performed in the Quivolgo catchment before the present wildfire condition (2014) using the carbon isotopic composition of fatty acids (CSSI fingerprint) to apportion sediment sources coming from roads and soils under pine plantations, native forest and riparian vegetation or buffer zone (Bravo-Linares et al. 2018). This study showed that unpaved roads were a major sediment source throughout the hydrological year. In the post-wildfire situation, road source contribution to sediments, as a proportion, was only important at the end of the rainy period (October 2017), indicating that fire switched on a new sediment source immediately after the rainy period started, i.e. rill erosion, which dominated and overprinted the “background” contribution from roads. This implies a substantially greater volume of sediment mobilised from sub-surface compared to roads during the rainy period post-fire.

The mixing model apportionment showed a strong negative correlation between sub-surface and road global posterior distributions ( $r = -0.71$ , Supplementary Figure 2) indicating that contribution of one source could be trading off against the other (Parnell et al. 2010, 2013). The reason for this has been attributed to the similarities between sources being evaluated. In this case, it is possible to link the similarity between these two sources to mobilisation of sub-surface material into roads. Nevertheless, this mixing process was avoided by taking samples at the opposite side of forest slopes. When there is evidence that can support similarities between two or more sources (e.g. field observations, physical processes), data can be combined either a priori or a posteriori (Phillips et al. 2014; Stock et al. 2018; Upadhayay et al. 2018). However, the posterior source

distribution aggregation ability of MixSIAR mixing model requires careful consideration when using it in sediment apportionment. In our case, we did not find sufficient plausible reasons to support the sub-surface and road posterior source distribution aggregation, even when it was possible relying on frequentist statistical testing that showed no significant differences between these two sources in nine of ten tracers used in source apportionment (Stock et al. 2018). Other studies under coniferous tree cover have reported subsoil as the dominant sediment source after wildfire using  $^{137}\text{Cs}$  and  $^{210}\text{Pb}_{\text{ex}}$  as tracers, including channel banks as part of the subsoil source group because of its similar radionuclide composition (Owens et al. 2012). Here, the inclusion of geochemical tracers in the unmixing process allowed sub-surface soil material to be distinguished from channel bank material. This was despite similarities in terms of  $^{210}\text{Pb}_{\text{ex}}$  and geochemical composition, with low global posterior distribution correlation between them ( $r = -0.2$ , Supplementary Figure 2) demonstrating that, for both sources, posterior distributions from the mixing model output are distinguishable (Parnell et al. 2010; Phillips et al. 2014).

#### 4.3.3 Post-fire apportionment considerations and limitations

The application of sediment fingerprinting technology in burnt commercial forest catchments is a valuable tool for forest managers to reveal sources that could contribute sediments to waterbodies and processes therein. To our knowledge, this is the first study that explores the tracer selection procedure based on the exclusion of non-conservative tracers in sediment source apportionment immediately after a wildfire in a catchment with forest plantations. However, there are some limitations in our study that should be addressed in the future: (1) The number of samples per source category should be increased in order to account adequately spatial variability, especially at surface and channel bank source categories, where we found

substantial variability in FRN activity and in geochemical element concentrations. (2) The low discriminatory capacity among sources (as shown by PCA plot, Fig. 8) when selecting tracers via exclusion of non-conservative tracers (Smith et al. 2018), although comparison with the classical tracer selection procedure (which maximise differences between source categories) did not show differences in terms of the dominant sources contributing to the weir. In fact, this process included one tracer, Cl, that showed important correlation with SSA and SOM content and wider posterior probability distributions than the method applied in this study, and (3) we encourage the application of tracer selection procedure based on the exclusion of non-conservative tracers in burnt landscapes knowing the implication that SOM and SSA alterations could have in tracer properties. Additionally, testing model and tracer accuracy and precision with artificial mixtures is advised in order to improve source discrimination capacity and the quality of mixing model outputs.

## 5 Conclusions

Sediment sources within a forest catchment affected by wildfire were assessed using the MixSIAR mixing model. The exploration of environmental radionuclides together with geochemical elements, through a selection procedure based on the examination of tracer conservative behaviour, led to ten fingerprinting properties (1 FRN and 9 geochemical elements) being used in sediment apportionment within a wildfire forest catchment context. The tracers that passed the selection criteria demonstrated their suitability to be used due to the following reasons: (i) weak and non-significant linear relationship between tracer concentrations and SSA and SOM, thereby negligible alteration of tracer properties due to enrichment or depletion, and (ii) conservative behaviour supported by the inclusion of sediment samples within source convex hull boundaries for all tracer combinations.

The dominant sediment source during the first two periods evaluated was shallow sub-surface soil (2–4 cm), demonstrating a shift in the dominant sediment source in the forest catchment after being affected by a wildfire, and the main drivers of sediment release were the overland flow and consequent rill erosion that occurred immediately after the rainy period started. In addition, forest road contribution was also important, especially during the last period evaluated, which has been reported by other studies in non-fire-affected forested catchments. However, considerations should be given to (1) the strong negative correlation between the sub-surface soil and forest road global posterior distributions found in the mixing model apportionment, (2) the sample size of some source categories

e.g. channel banks and (3) the low discrimination capacity of the selected tracers.

Finally, climate change and land use transformation into massive plantations of exotic tree species can increase wildfire frequency which in turn creates landscapes that are more vulnerable to erosion processes. The increase in the number of wildfires in Chile will generate a sustained source of sediment release into waterbodies, especially during rainy events with consequences for water supply and hydropower production. Early post-fire targeting and management of the potential sediment sources in forested catchment can reduce the off-site impacts of ashes and sediments released after rainy episodes. Herein, sediment fingerprinting can become an affordable tool for forest companies to assess and develop focalised strategies when attempting to face soil erosion problems and its downstream impacts that are risen after a wildfire event.

**Supplementary Information** The online version contains supplementary material available at <https://doi.org/10.1007/s11368-021-02943-w>.

**Acknowledgements** We would like to dedicate this study to all people that lost their possessions during this wildfire that affected a vast territory in Central Chile. The authors also want to acknowledge the logistic support of Bioforest to perform the study in the Quivolgo catchment. Finally, we would like to acknowledge the valuable comments from the reviewers that greatly improved the quality of this manuscript.

**Availability of data and material** The electronic supplementary material can be seen in the Supplementary information of this article.

**Code availability** Not applicable.

**Author contribution** Enrique Muñoz-Arcos, Claudio Bravo-Linares, Ramón Bustamante-Ortega and William H. Blake contributed to the study conception and design. Material preparation, sampling, data collection and analysis were performed by Enrique Muñoz-Arcos, Claudio Bravo-Linares, Luis Ovando-Fuentealba, Ramón Bustamante-Ortega, Alejandra Castillo-Santana, Alicia Cuevas-Aedo and Alex Taylor. The first draft of the manuscript was written by Enrique Muñoz-Arcos and all authors commented on previous versions of the manuscript. All authors read and approved the final version of this manuscript.

**Funding** This research in the Quivolgo catchment was supported and financed by Bioforest, Arauco.

## Declarations

**Conflict of interest** The authors declare no competing interests.

## References

- Appleby PG (2001) Chronostratigraphic techniques in recent sediments. In: Last WM, Smol JP (eds) Tracking environmental change using lake sediments: basin analysis, coring, and chronological techniques. Springer Netherlands, Dordrecht, pp 171–203

- Blake WH, Wallbrink PJ, Doerr SH et al (2006a) Magnetic enhancement in wildfire-affected soil and its potential for sediment-source ascription. *Earth Surf Process Landf* 31:249–264. <https://doi.org/10.1002/esp.1247>
- Blake WH, Wallbrink PJ, Doerr SH, et al (2006b) Using geochemical stratigraphy to indicate post-fire sediment and nutrient fluxes into water supply reservoir, Sydney, Australia. Wallingford : IAHS
- Blake WH, Droppo IG, Humphreys GS et al (2007) Structural characteristics and behavior of fire-modified soil aggregates. *J Geophys Res-Earth Surf* 112:F02020. <https://doi.org/10.1029/2006JF000660>
- Blake WH, Wallbrink PJ, Droppo IG (2009a) Sediment aggregation and water quality in wildfire-affected river basins. *Mar Freshw Res* 60: 653–659. <https://doi.org/10.1071/MF08068>
- Blake WH, Wallbrink PJ, Wilkinson SN et al (2009b) Deriving hillslope sediment budgets in wildfire-affected forests using fallout radionuclide tracers. *Geomorphology* 104:105–116. <https://doi.org/10.1016/j.geomorph.2008.08.004>
- Blake WH, Theocharopoulos SP, Skoulikidis N et al (2010) Wildfire impacts on hillslope sediment and phosphorus yields. *J Soils Sediments* 10:671–682. <https://doi.org/10.1007/s11368-010-0201-y>
- Bodi MB, Martin DA, Balfour VN et al (2014) Wildland fire ash: production, composition and eco-hydro-geomorphic effects (vol 130, pg 103, 2014). *Earth-Sci Rev* 138:503–503. <https://doi.org/10.1016/j.earscirev.2014.07.005>
- Brandt C, Dercon G, Cadisch G et al (2018) Towards global applicability? Erosion source discrimination across catchments using compound-specific delta C-13 isotopes. *Agric Ecosyst Environ* 256:114–122. <https://doi.org/10.1016/j.agee.2018.01.010>
- Bravo-Linares C, Schuller P, Castillo A et al (2018) First use of a compound-specific stable isotope (CSSI) technique to trace sediment transport in upland forest catchments of Chile. *Sci Total Environ* 618:1114–1124. <https://doi.org/10.1016/j.scitotenv.2017.09.163>
- Bravo-Linares C, Schuller P, Castillo A et al (2020) Combining isotopic techniques to assess historical sediment delivery in a forest catchment in central Chile. *J Soil Sci Plant Nutr* 20:83–94. <https://doi.org/10.1007/s42729-019-00103-1>
- Carmona A, Gonzalez ME, Nahuelhual L, Silva J (2012) Spatio-temporal effects of human drivers on fire danger in Mediterranean Chile. *Bosque* 33:321–328. <https://doi.org/10.4067/S0717-92002012000300016>
- Certini G (2005) Effects of fire on properties of forest soils: a review. *Oecologia* 143:1–10. <https://doi.org/10.1007/s00442-004-1788-8>
- Collins AL, Walling DE (2002) Selecting fingerprint properties for discriminating potential suspended sediment sources in river basins. *Journal of hydrology (Amsterdam)* 261:218–244. [https://doi.org/10.1016/S0022-1694\(02\)00011-2](https://doi.org/10.1016/S0022-1694(02)00011-2)
- Collins AL, Pulley S, Foster IDL et al (2017) Sediment source fingerprinting as an aid to catchment management: a review of the current state of knowledge and a methodological decision-tree for end-users. *J Environ Manag* 194:86–108. <https://doi.org/10.1016/j.jenvman.2016.09.075>
- Collins AL, Blackwell M, Boeckx P et al (2020) Sediment source fingerprinting: benchmarking recent outputs, remaining challenges and emerging themes. *J Soils Sediments* 20:4160–4193. <https://doi.org/10.1007/s11368-020-02755-4>
- Core Team R (2018) R: a language and environment for statistical computing. Austria, Vienna
- de la Barrera F, Barraza F, Favier P et al (2018) Megafires in Chile 2017: monitoring multiscale environmental impacts of burned ecosystems. *Sci Total Environ* 637:1526–1536. <https://doi.org/10.1016/j.scitotenv.2018.05.119>
- DeBano LF (2000) The role of fire and soil heating on water repellency in wildland environments: a review. *J Hydrol* 231:195–206. [https://doi.org/10.1016/S0022-1694\(00\)00194-3](https://doi.org/10.1016/S0022-1694(00)00194-3)
- Dyrness CT, Youngberg CT (1957) The effect of logging and slash-burning on soil structure. *Soil Sci Soc Am J* 21:444–447. <https://doi.org/10.2136/sssaj1957.03615995002100040022x>
- Estrany J, Lopez-Tarazon JA, Smith HG (2016) Wildfire effects on suspended sediment delivery quantified using fallout radionuclide tracers in a Mediterranean catchment. *Land Degrad Dev* 27:1501–1512. <https://doi.org/10.1002/ldr.2462>
- FAO (2020) Global Forest Resources Assessment 2020: Main Report. Rome.
- Garcia-Comendador J, Martinez-Carreras N, Fortesa J et al (2020) Analysis of post-fire suspended sediment sources by using colour parameters. *Geoderma* 379:114638. <https://doi.org/10.1016/j.geoderma.2020.114638>
- Garcia-Corona R, Benito E, de Blas E, Varela ME (2004) Effects of heating on some soil physical properties related to its hydrological behaviour in two north-western Spanish soils. *Int J Wildland Fire* 13:195–199. <https://doi.org/10.1071/WF03068>
- Gomez-Gonzalez S, Gonzalez ME, Paula S et al (2019) Temperature and agriculture are largely associated with fire activity in Central Chile across different temporal periods. *For Ecol Manag* 433:535–543. <https://doi.org/10.1016/j.foreco.2018.11.041>
- González ME, Lara A, Urrutia R, Bosnich J (2011) Cambio climático y su impacto potencial en la ocurrencia de incendios forestales en la zona centro-sur de Chile (33° - 42° S). *Bosque (Valdivia)* 32:215–219
- Gonzalez ME, Gomez-Gonzalez S, Lara A et al (2018) The 2010-2015 Megadrought and its influence on the fire regime in central and south-central Chile. *Ecosphere* 9:e02300. <https://doi.org/10.1002/ecs2.2300>
- Ice GG, Neary DG, Adams PW (2004) Effects of wildfire on soils and watershed processes. *J For* 102:16–20
- INFOR (2020) Chilean Statistical Yearbook of Forestry 2020
- Johansen MP, Hakonson TE, Whicker FW, Breshears DD (2003) Pulsed redistribution of a contaminant following forest fire: Cesium-137 in runoff. *J Environ Qual* 32:2150–2157
- Kassambara A, Fabian M (2019) factoextra: extract and visualize the results of multivariate data analyses. Version 1.0.6
- Koiter AJ, Owens PN, Petticrew EL, Lobb DA (2013) The behavioural characteristics of sediment properties and their implications for sediment fingerprinting as an approach for identifying sediment sources in river basins. *Earth-Sci Rev* 125:24–42. <https://doi.org/10.1016/j.earscirev.2013.05.009>
- Koiter AJ, Owens PN, Petticrew EL, Lobb DA (2018) Assessment of particle size and organic matter correction factors in sediment source fingerprinting investigations: an example of two contrasting watersheds in Canada. *Geoderma* 325:195–207. <https://doi.org/10.1016/j.geoderma.2018.02.044>
- Kraushaar S, Schumann T, Ollesch G et al (2015) Sediment fingerprinting in northern Jordan: element-specific correction factors in a carbonatic setting. *J Soils Sediments* 15:2155–2173. <https://doi.org/10.1007/s11368-015-1179-2>
- Lacey JP, Evrard O, Smith HG et al (2017) The challenges and opportunities of addressing particle size effects in sediment source fingerprinting: a review. *Earth-Sci Rev* 169:85–103. <https://doi.org/10.1016/j.earscirev.2017.04.009>
- Lê S, Josse J, Husson F (2008) FactoMineR: an R package for multivariate analysis. *J Stat Softw* 25:18
- Lizaga I, Latorre B, Gaspar L, Navas A (2020) FingerPro: an R package for tracking the provenance of sediment. *Water Resour Manag* 34: 3879–3894. <https://doi.org/10.1007/s11269-020-02650-0>
- Martin DA (2016) At the nexus of fire, water and society. *Philos Trans R Soc B-Biol Sci* 371:20150172. <https://doi.org/10.1098/rstb.2015.0172>
- Mazzorana B, Picco L, Rainato R et al (2019) Cascading processes in a changing environment: disturbances on fluvial ecosystems in Chile and implications for hazard and risk management. *Sci Total Environ* 655:1089–1103. <https://doi.org/10.1016/j.scitotenv.2018.11.217>



- McWethy DB, Pauchard A, Garcia RA et al (2018) Landscape drivers of recent fire activity (2001–2017) in south-central Chile. *PLoS One* 13:e0201195. <https://doi.org/10.1371/journal.pone.0201195>
- Moody JA, Shakesby RA, Robichaud PR et al (2013) Current research issues related to post-wildfire runoff and erosion processes. *Earth-Sci Rev* 122:10–37. <https://doi.org/10.1016/j.earscirev.2013.03.004>
- Motha JA, Wallbrink PJ, Hairsine PB, Grayson RB (2003) Determining the sources of suspended sediment in a forested catchment in south-eastern Australia. *Water Resour Res* 39:1056. <https://doi.org/10.1029/2001WR000794>
- Oros DR, Mazurek MA, Baham JE, Simoneit BRT (2002) Organic tracers from wild fire residues in soils and rain/river wash-out. *Water Air Soil Pollut* 137:203–233. <https://doi.org/10.1023/A:1015557301467>
- Owens PN, Blake WH, Petticrew EL (2006) Changes in sediment sources following wildfire in mountainous terrain: a paired-catchment approach, British Columbia, Canada. In: Kronvang B, Faganeli J, Ogrinc N (eds) *The interactions between sediments and water*. Springer Netherlands, Dordrecht, pp 273–281
- Owens PN, Blake WH, Giles TR, Williams ND (2012) Determining the effects of wildfire on sediment sources using Cs-137 and unsupported Pb-210: the role of landscape disturbances and driving forces. *J Soils Sediments* 12:982–994. <https://doi.org/10.1007/s11368-012-0497-x>
- Owens PN, Blake WH, Gaspar L et al (2016) Fingerprinting and tracing the sources of soils and sediments: earth and ocean science, geoarchaeological, forensic, and human health applications. *Earth-Sci Rev* 162:1–23. <https://doi.org/10.1016/j.earscirev.2016.08.012>
- Palazon L, Navas A (2017) Variability in source sediment contributions by applying different statistic test for a Pyrenean catchment. *J Environ Manag* 194:42–53. <https://doi.org/10.1016/j.jenvman.2016.07.058>
- Parnell AC, Inger R, Bearhop S, Jackson AL (2010) Source partitioning using stable isotopes: coping with too much variation. *PLoS One* 5:e9672. <https://doi.org/10.1371/journal.pone.0009672>
- Parnell AC, Phillips DL, Bearhop S et al (2013) Bayesian stable isotope mixing models. *Environmetrics* 24:387–399. <https://doi.org/10.1002/env.2221>
- Phillips DL, Inger R, Bearhop S et al (2014) Best practices for use of stable isotope mixing models in food-web studies. *Can J Zool* 92:823–835. <https://doi.org/10.1139/cjz-2014-0127>
- Robinne F-N, Hallema DW, Bladon KD, Buttle JM (2020) Wildfire impacts on hydrologic ecosystem services in North American high-latitude forests: a scoping review. *J Hydrol* 581:124360. <https://doi.org/10.1016/j.jhydrol.2019.124360>
- RStudio Team (2015) *RStudio: integrated development for R*. RStudio, Inc., Boston, MA.
- Rust AJ, Randell J, Todd AS, Hogue TS (2019) Wildfire impacts on water quality, macroinvertebrate, and trout populations in the Upper Rio Grande. *For Ecol Manag* 453:117636. <https://doi.org/10.1016/j.foreco.2019.117636>
- Shakesby RA, Doerr SH (2006) Wildfire as a hydrological and geomorphological agent. *Earth-Sci Rev* 74:269–307. <https://doi.org/10.1016/j.earscirev.2005.10.006>
- Shakesby RA, Moody JA, Martin DA, Robichaud PR (2016) Synthesising empirical results to improve predictions of post-wildfire runoff and erosion response. *Int J Wildland Fire* 25:257–261. <https://doi.org/10.1071/WF16021>
- Smith HG, Blake WH (2014) Sediment fingerprinting in agricultural catchments: a critical re-examination of source discrimination and data corrections. *Geomorphology* 204:177–191. <https://doi.org/10.1016/j.geomorph.2013.08.003>
- Smith HG, Sheridan GJ, Lane PNJ et al (2011a) Wildfire effects on water quality in forest catchments: a review with implications for water supply. *J Hydrol* 396:170–192. <https://doi.org/10.1016/j.jhydrol.2010.10.043>
- Smith HG, Sheridan GJ, Lane PNJ et al (2011b) Changes to sediment sources following wildfire in a forested upland catchment, south-eastern Australia. *Hydrol Process* 25:2878–2889. <https://doi.org/10.1002/hyp.8050>
- Smith HG, Blake WH, Owens PN (2013) Discriminating fine sediment sources and the application of sediment tracers in burned catchments: a review. *Hydrol Process* 27:943–958. <https://doi.org/10.1002/hyp.9537>
- Smith HG, Karam DS, Lennard AT (2018) Evaluating tracer selection for catchment sediment fingerprinting. *J Soils Sediments* 18:3005–3019. <https://doi.org/10.1007/s11368-018-1990-7>
- Stock BC, Semmens BX (2018) *MixSIAR GUI User Manual*. Version 3.1. <https://doi.org/10.5281/zenodo.47719>
- Stock BC, Jackson AL, Ward EJ et al (2018) Analyzing mixing systems using a new generation of Bayesian tracer mixing models. *PeerJ* 6:e5096. <https://doi.org/10.7717/peerj.5096>
- Stone M, Collins AL, Silins U et al (2014) The use of composite fingerprints to quantify sediment sources in a wildfire impacted landscape, Alberta, Canada. *Sci Total Environ* 473:642–650. <https://doi.org/10.1016/j.scitotenv.2013.12.052>
- Taylor KT, Maxwell BD, McWethy DB et al (2017) *Pinus contorta* invasions increase wildfire fuel loads and may create a positive feedback with fire. *Ecology* 98:678–687. <https://doi.org/10.1002/ecy.1673>
- Upadhayay HR, Smith HG, Griepentrog M et al (2018) Community managed forests dominate the catchment sediment cascade in the mid-hills of Nepal: a compound-specific stable isotope analysis. *Sci Total Environ* 637:306–317. <https://doi.org/10.1016/j.scitotenv.2018.04.394>
- Urrutia-Jalabert R, Gonzalez ME, Gonzalez-Reyes A et al (2018) Climate variability and forest fires in central and south-central Chile. *Ecosphere* 9:e02171. <https://doi.org/10.1002/ecs2.2171>
- Venables WN, Ripley BD (2002) *Modern applied statistics with S*, Fourth. Springer, New York
- Walling DE (2013) The evolution of sediment source fingerprinting investigations in fluvial systems. *J Soils Sediments* 13:1658–1675. <https://doi.org/10.1007/s11368-013-0767-2>
- Wilkinson SN, Wallbrink PJ, Hancock GJ et al (2009) Fallout radionuclide tracers identify a switch in sediment sources and transport-limited sediment yield following wildfire in a eucalypt forest. *Geomorphology* 110:140–151. <https://doi.org/10.1016/j.geomorph.2009.04.001>
- Williams CHS, Silins U, Spencer SA et al (2019) Net precipitation in burned and unburned subalpine forest stands after wildfire in the northern Rocky Mountains. *Int J Wildland Fire* 28:750–760. <https://doi.org/10.1071/WF18181>
- WMO (1994) *Guide to hydrological practices*, 5th edn

**Publisher's note** Springer Nature remains neutral with regard to jurisdictional claims in published maps and institutional affiliations.